Clinical Cancer Research

Inhibition of REDD1 Sensitizes Bladder Urothelial Carcinoma to Paclitaxel by Inhibiting Autophagy

Qinghai Zeng[1], Jianye Liu[2], Peiguo Cao[3], Jingjing Li[4], Xiaoming Liu[5], Xiaojun Fan[6], Ling Liu[7], Yan Cheng[8], Wei Xiong[9], Jigang Li[10], Hao Bo[11], Yuxing Zhu[3], Fei Yang[12], Jun Hu[13], Ming Zhou[9], Yanhong Zhou[9], Qiong Zou[14], Jianda Zhou[4], and Ke Cao[3]

Abstract

Purpose: Regulated in development and DNA damage response-1 (REDD1) is a stress-related protein and is involved in the progression of cancer. The role and regulatory mechanism of REDD1 in bladder urothelial carcinoma (BUC), however, is yet unidentified.

Experimental Design: The expression of REDD1 in BUC was detected by Western blot analysis and immunohistochemistry (IHC). The correlation between REDD1 expression and clinical features in patients with BUC were assessed. The effects of REDD1 on cellular proliferation, apoptosis, autophagy, and paclitaxel sensitivity were determined both *in vitro* and *in vivo*. Then the targeted-regulating mechanism of REDD1 by miRNAs was explored.

Results: Here the significant increase of REDD1 expression is detected in BUC tissue, and REDD1 is first reported as an independent prognostic factor in patients with BUC. Silencing REDD1 expression in T24 and EJ cells decreased cell proliferation, increased apoptosis, and decreased autophagy, whereas the ectopic expression of REDD1 in RT4 and BIU87 cells had the opposite effect. In addition, the REDD1-mediated proliferation, apoptosis, and autophagy are found to be negatively regulated by miR-22 *in vitro*, which intensify the paclitaxel sensitivity via inhibition of the well-acknowledged REDD1–EEF2K–autophagy axis. AKT/mTOR signaling initially activated or inhibited in response to silencing or enhancing REDD1 expression and then recovered rapidly. Finally, the inhibited REDD1 expression by either RNAi or miR-22 sensitizes BUC tumor cells to paclitaxel in a subcutaneous transplant carcinoma model *in vivo*.

Conclusions: REDD1 is confirmed as an oncogene in BUC, and antagonizing REDD1 could be a potential therapeutic strategy to sensitize BUC cells to paclitaxel. *Clin Cancer Res; 24(2); 445–59. ©2017 AACR.*

Introduction

Bladder urothelial carcinoma (BUC) is one of the most common malignant tumors of the urinary system and is characterized by rapid progression and a high rate of recurrence (1, 2). BUC recurs in approximately 50% of patients after surgery, and the 5-year overall survival rate for patients who develop or present with metastatic disease is a dismal 6% (3). Combination chemotherapy has been shown to reduce the recurrence rate of BUC and to improve patients' survival (4). Treatment with the microtubule stabilizing agent, paclitaxel has also proven to be an effective therapy against BUC (5, 6). Recent phase III clinical trials have found that a PCG (paclitaxel plus cisplatin plus gemcitabine) regimen, consisting of the addition of paclitaxel to a standard chemotherapy regimen of cisplatin plus gemcitabine (GC), can improve the overall response rate and overall survival rate of patients with BUC (7). However, acquired or *de novo* resistance to paclitaxel limits its clinical application in the treatment of BUC, and the identification of approaches to sensitize BUC to paclitaxel remains a significant clinical challenge (8, 9).

Autophagy is an important mechanism of resistance to chemotherapy, and can help tumor cells overcome metabolic stress caused by chemotherapeutic drugs like paclitaxel, resulting in survival of cancer cells and development of therapeutic resistance (10, 11). REDD1 is a stress-related protein; its expression is induced under hypoxia, stress, and following DNA damage (12). REDD1 participates in autophagy induction through

[1]Department of Dermatology, Third Xiangya Hospital, Central South University, Changsha, Hunan, P.R. China. [2]Department of Urology, Third Xiangya Hospital, Central South University, Changsha, Hunan, P.R. China. [3]Department of Oncology, Third Xiangya Hospital, Central South University, Changsha, Hunan, P.R. China. [4]Department of Plastic Surgery, Third Xiangya Hospital, Central South University, Changsha, Hunan, P.R. China. [5]Department of Gastroenterology, Third Xiangya Hospital, Central South University, Changsha, Hunan, P.R. China. [6]Research Service Office, Third Xiangya Hospital, Central South University, Changsha, Hunan, P.R. China. [7]Outpatient service office, Third Xiangya Hospital, Central South University, Changsha, Hunan, P.R. China. [8]Department of Pharmacology, School of Pharmaceutical Sciences, Central South University, Changsha, Hunan, P.R. China. [9]Cancer Research Institute and Key Laboratory of Carcinogenesis of Ministry of Health, Central South University, Changsha, Hunan, P.R. China. [10]Department of Pathology, Hunan Cancer Hospital and The Affiliated Cancer Hospital of Xiangya School of Medicine, Central South University, Changsha, Hunan, P.R. China. [11]Institute of Reproductive and Stem Cell Engineering, Central South University, Changsha, Hunan, P.R. China. [12]School of Public Health, Central South University, Changsha, Hunan, P.R. China. [13]Department of Tissue-bank, Hunan Cancer Hospital and The Affiliated Cancer Hospital of Xiangya School of Medicine, Central South University, Changsha, Hunan, P.R. China. [14]Department of Pathology, Third Xiangya Hospital, Central South University, Changsha, Hunan, P.R. China.

Note: Supplementary data for this article are available at Clinical Cancer Research Online (http://clincancerres.aacrjournals.org/).

Q. Zeng, J. Liu, and P. Cao contributed equally to this article.

Corresponding Author: Ke Cao, Third Xiangya Hospital, Central South University, Changsha 410013, China. Phone: 0731-88618930; Fax: 86-0731-88618936; E-mail: CSUcaoke@163.com

doi: 10.1158/1078-0432.CCR-17-0419

Translational Relevance

Regulated in development and DNA damage response-1 (REDD1) is involved in the development and progression of cancer. However, the role and regulatory mechanism of REDD1 in bladder urothelial carcinoma (BUC) is not explored. Here, we describe that REDD1 has significantly elevated expression in BUC tissue, and high REDD1 expression was correlated with poorer survival of patients with bladder urothelial cancer. Functional analysis reveals that REDD1 participates in regulating proliferation, apoptosis, and autophagy in BUC cells. In addition, we show that silencing the REDD1–EEF2K–autophagy axis increased the sensitivity of BUC cells to paclitaxel, while activating this axis reduced BUC paclitaxel sensitivity. We further demonstrate that REDD1-mediated proliferation, apoptosis, and autophagy is negatively regulated by miR-22, and that miR-22 sensitizes BUC cells to paclitaxel by inhibiting the REDD1–EEF2K–autophagy axis. In conclusion, REDD1 acts as an oncogene in BUC, and antagonizing REDD1 could be a potential therapeutic strategy to sensitize BUC cells to paclitaxel.

the mTOR–EEF2K pathway (13). It has been reported that REDD1-induced autophagy promotes development of drug resistance in myeloma cells (14), and prostate cancer cells (15). As an inhibitor of the mTOR pathway, REDD1 is involved in the regulation of cell growth, tumorigenesis, and cell aging (16, 17). REDD1 owns tissue-specific pattern acting as an oncogene in ovarian cancer (18, 19) and prostate cancer (20), whereas a tumor suppressor in non–small cell lung cancer (21) and breast cancer (22). However, the involvement of REDD1 and its clinical/prognostic significance in BUC are unclear. Here we investigate the expression of REDD1 in BUC and its underlying role in the pathogenesis of BUC; we also explore the impact of REDD1-mediated autophagy on BUC resistance to paclitaxel treatment.

Materials and Methods

Tissue and cell lines

Human primary BUC tissues, the corresponding adjacent noncancerous bladder urothelial tissues and paraffin-embedded specimens of BUC were collected at the Third Xiangya Hospital of Central South University and Hunan Cancer Hospital from 2004 to 2016. All patients with BUC were histopathologically and clinically diagnosed and were treated with radical cystectomy. For the use of these clinical materials for research purposes, prior patient consent and approval from the Institutional Research Ethics Committee were obtained. Clinical information of 112 paraffin-embedded specimens of BUC samples is described in detail in Table 1. Human BUC cell lines (BIU-87, 5637, T24, EJ, and RT4) were purchased from ATCC and maintained in DMEM supplemented with 10% FBS, 1% penicillin/streptomycin at 37°C under an atmosphere of 5% CO_2. The studies were conducted in accordance with the following ethical guidelines: Declaration of Helsinki, International Ethical Guidelines for Biomedical Research Involving Human Subjects (CIOMS), Belmont Report, and U.S. Common Rule.

Immunostaining

The tissues embedded in paraffin were cut into 5-μm slides. Sections were dewaxed in xylene, rehydrated with graded alcohols, treated with 0.3% H_2O_2 in methanol, and blocked with 1% bovine serum albumin (BSA). Sections were incubated with anti-REDD1 (1:200, Merckmillipore, ABC245) at 4°C overnight. After addition of polymer enhancer, the sections were treated with peroxidase-labeled streptavidin for 30 minutes at room temperature. The antibody reaction was visualized using a fresh substrate solution containing 3,3′-diaminobenzidine tetrahydrochloride (DAB). Sections were counter-stained with hematoxylin, dehydrated, and mounted in glycerol-vinyl-alcohol (GVA mount; Zymed).

The degree of immunostaining of formalin-fixed, paraffin-embedded sections was reviewed and scored separately by two independent pathologists uninformed of the histopathological features and patient data of the samples. Scores were determined by combining the proportion of positively stained tumor cells and the intensity of staining. Tumor cell proportions were scored as follows: 0 (no positive tumor cells); 1 (<10% positive tumor cells); 2 (10%–35% positive tumor cells); 3 (35%–75% positive tumor cells); and 4 (>75% positive tumor cells). Staining intensity was graded according to the following standard: 1 (no staining); 2 (weak staining = light yellow); 3 (moderate staining = yellow brown); and 4 (strong staining = brown). The staining index was calculated as the product of the staining intensity score and the proportion of positive tumor cells. Using this method of assessment, the expression of REDD1 in BUC was evaluated by the staining index (scored as 0, 1, 2, 3, 4, 6, 8, 9, or 12). Staining index scores $\geq$6 were identified as high expression, while scores <6 were considered low expression.

Cell transfection

miR-22-mimics/inhibitors, REDD1-shRNAs, plasmids for overexpression of REDD1, and negative controls were purchased from GeneChem Biotechnology Company. Cells were transfected as previously described (23–25). BUC cells were seeded in 6-well plates and allowed to reach 70% confluence after 24 hours. Lipofectamine 3000 (Thermo Fisher Scientific) was used to transfect cells with DNA complexes according to manufacturer's instruction. Cells were harvested for RNA extraction and protein extraction 24 and 48 hours after transfection, respectively.

Quantitative real-time PCR

RNA was extracted from cells using Trizol, according to the manufacturer (GenStar). RNA purity was assessed by spectrophotometry (A260/A280 > 1.8). Single-stranded cDNAs were generated using M-MLV transcriptase (Promega) following the manufacturer's directions. Real-time quantitative PCR for expression of miR-22 and REDD1 mRNA expression were performed using SYBR Green PCR Master Mix according to the manufacturer's protocol. Triplicate PCR amplifications were performed for each sample. The relative gene expression to control was determined by the standard $2^{-\Delta\Delta C_t}$ method. β-Actin or U6 was used as internal control. The primer sequences for amplification of miR-22 were as follows: forward: 5′-GTAGTTCTTCAGTGGCAA-3′; reverse: 5′-TTTGGCACTAGCACATT-3′. The primer sequences for REDD1 were as follows: forward: 5′-GACAGCAGCAACAGTGGCTTC-3′; reverse: 5′- CCACGCTATGGCAGCTCTTGC-3′.

Western blot analysis

Tissues and cells were washed with PBS and then lysed with RIPA lysis buffer containing 10% protease inhibitor cocktail (Roche) on ice for 30 minutes. Protein concentrations were determined using a BCA Protein Assay Reagent Kit (Thermo Scientific). Aliquots of cell lysates containing 20 to 40 μg protein were separated by 10% SDS-polyacrylamide gel and transferred to PVDF membranes. Membranes were blocked with TBST buffer containing 5% skim milk, incubated with anti-REDD1 (1:1,000 Merckmillipore, ABC245), anti-cleaved caspase 3 (1:1,000 Proteintech, 19677-1-AP), anti-cleaved PARP (1:1,000, Abcam, ab4830), anti-EEF2K (1:1,000, Abcam, ab4830), anti-LC3 (1:2,000, Abcam, ab51520), anti-AKT (1:1,000, Abcam, ab8805), anti-p-AKT(Ser473) (Abcam, ab81283), anti-mTOR (1:1,000, CST, #2972), anti-p-mTOR(Ser2448) (CST, #2971), anti-S6K1 (1:5,000, Abcam, ab32529), anti- p-S6K1(p-T389) (1:1,000, Abcam, ab2571), and anti-β-actin (1:1,000, Santa Cruz, sc-47778) at 4°C overnight, followed by the addition of horseradish peroxidase-linked anti-mouse IgG secondary antibodies and ECL visualization of the bands. Quantification of the bands was carried out using densitometric analysis software, Quantity One (Bio-Rad), and processed as described previously (Bio-Rad). The expression of β-actin was used as an internal control to normalize the expressions of other proteins.

Cell proliferation assay

Parental T24, EJ, BIU87, and RT4 cells, as well as T24, EJ, BIU87, or RT4 cells transfected with siRNA or plasmid were seeded in 96-well plates. Cell proliferation was determined using a commercial CCK-8 Assay Kit (Beyotime, #C0038) according to the manufacturer's instructions 72 hours after transfecting. The cells should be pretreated with autophagy inhibitors 3-methyladenine (3-MA, 10 mmol/L, sigma) or chloroquine diphosphate salt (CQ, 20 μmol/L, sigma) for 1 hour before other treatments if necessary. All assays were performed in triplicate.

Cell cycle and apoptosis assays

Parental T24, EJ, BIU87, and RT4 cells, as well as T24, EJ, BIU87, or RT4 cells transfected with siRNA or plasmid were seeded in six-well plates. Cells were treated with Taxol (paclitaxel) for 48 hours and harvested by centrifugation. Cell cycle and apoptosis assays was performed by FACS using a cell-cycle Detection Kit (Sigma) and Annexin V-FITC/PI Staining Kit (Mbchem) according to manufacturer's instructions. The proliferation index (PI) was calculated as followed: $PI = (S + G_2\text{–}M)/(S + G_2\text{–}M + G_0\text{–}G_1)$. All tests were performed in triplicate.

Clonogenic assay

Parental T24 and RT4 cells, as well as T24 or RT4 cells transfected with siRNA or plasmid were seeded in six-well plate without soft agar at 1,000 cells/well. Taxol was added to the plate for the Taxol treatment group. The cells were incubated for 2 weeks, and culture media was replaced at 2- to 3-day intervals. Cells were washed with PBS twice before harvest. The cells were fixed with 1 mL paraformaldehyde for 30 minutes. Fixed cells were stained with hematoxylin and counted under a microscope. Colonies of more than 50 cells were counted for all clonogenic assays.

Immunofluorescence staining

Parental T24, EJ, BIU87, and RT4 cells, as well as T24, EJ, BIU87, or RT4 cells transfected with siRNA or plasmid were grown on glass coverslips in 6-well plates. After cells grew to cover the glass coverslips they were fixed with 4% paraformaldehyde for 30 minutes. Fixed cells were washed with PBS three times and then treated with 1% Triton-100 for 10 minutes, to enhance antibody penetration. Cells were pretreated with 10% normal goat serum for 30 minutes, and incubated with anti-LC3B (1:1000, Abcam, ab51520) at 4°C overnight. After washing in PBS, cells were incubated with second antibody (Alexa Fluor 555 Goat Anti-Rabbit IgG [H+L], 2 mg/mL, A21428) for 40 minutes at room temperature. Immunofluorescent images were recorded with an LeicaTCS-SP5 confocal laser scanning microscope (Heidelberg, Germany.) The integrated optical density (IOD) was calculated by Motic Fluo 1.0 software to represent the LC3B expression level.

Dual-luciferase experiment

For luciferase reporter experiments, the psiCHECK2-REDD1-3′-UTR/MUT1/MUT2 vectors were used. HEK293T cells were grown in six-well plates and cotransfected with psiCHECK2-REDD1-3′-UTR/MUT1/MUT2 vectors and hsamiR-22-mimics/hsa-miR-22-mimics-NC. At 48 hours posttransfection, firefly and renilla luciferase activities were evaluated using the Dual Luciferase Reporter Assay system (Promega). The relative luciferase activities were calculated by the ratio of firefly luciferase/renilla luciferase activity and normalized to that of the control cells. The luciferase reporter assay was performed as previously described (26).

Xenograft mouse model

All nude mice were inoculated subcutaneously on the right axillary fossa with 200 μL (1×10^6 cells) of shRNA-REDD1-transfected T24/EJ cells, pYr-LVX-pir-miR-22 transfected T24/EJ cells, REDD1-transfected RT4/BIU87 cells, miR-22-inhibition lentivirus transfected RT4/BIU87 cells, and control cells. When the animals developed palpable tumors, mice were administered 10 mg/ kg paclitaxel, diluted in PBS, by intraperitoneal injection twice a week. The size of the transplanted tumors was approximated every 3 days by measurement of tumor length (L) and width (W). All animals were sacrificed 35 days after inoculation and tumors were collected. The tumor volume (V) was calculated according to the formula $V = 1/2(L \times W^2)$. All animal work was approved by an ethics committee.

TUNEL staining

Apoptotic tumor cells were detected using a Tunel assay (Roche). Briefly, the transplanted tumors were fixed with 4% paraformaldehyde solution for 60 minutes. Then embedded in paraffin and cut into 5-μm slides. After being dewaxed, rehydrated, and repaired, the cells on the slides were permeabilized by permeabilization wash buffer. The slides were performed using mixture of TdT and dUTP at 37 °C for 120 minutes in a humidity chamber. Then the slides were treated with 0.3% H_2O_2 in methanol for 15 minutes. After being washed by PBS, the slides were added by converter-POD at 37°C for 30 minutes. Following incubation, excess labeling solution is washed off with PBS and the chromatin of apoptotic cell were visualized using DAB. Sections were then counter-stained with hematoxylin, dehydrated, and mounted in glycerol-vinyl-alcohol (GVA mount, Zymed). The degree of apoptosis was determined by combining the proportion of positively stained nuclei and the intensity of staining.

Statistical analysis

The statistical software package SPSS19.0 (SPSS incorporated, Chicago) was used for all statistical analysis. All experiments were performed in triplicate at the minimum. Data are presented as mean ± SD. Significance tests were conducted on the data groups using ANOVA followed by a comparison between the specific groups using the Student *t* test.

The relationship between REDD1 expression and the clinicopathological characteristics was tested by the χ^2 test. Survival curves were plotted according to the Kaplan–Meier method and compared by the log-rank test. Survival data were evaluated using univariate and multivariate Cox-regression analyses. $P < 0.05$ in all cases was considered statistically significant.

Results

Increased expression of REDD1 correlates with poor patient survival

Western blot analysis was carried out in eight pairs of human primary BUC tissues and their corresponding adjacent noncancerous bladder urothelial tissues. Compared with corresponding adjacent noncancerous tissues overexpression of REDD1 at the protein level was detected in 75.0% (6/8) of human primary BUCs (Fig. 1A). Those results were further confirmed by immunohistochemistry performed in parallel on the same eight tumor/normal pairs (Fig. 1B). Immunohistochemistry for REDD1 expression further was performed on paraffin sections from 112 primary BUC samples; 32 samples also had adjacent non-neoplastic bladder tissue samples available for comparison. REDD1 expression was significantly overexpressed in 32 BUC tissue compared with matched normal bladder tissue (Fig. 1C). Associations between REDD1 expression and clinicopathologic features of BUC were examined. REDD1 levels inversely correlated with advanced pT ($P = 0.011$, Table 1) and pN classification ($P < 0.001$; Table 1). There were no significant associations between REDD1 expression and other clinicopathologic features of BUC, including patient age, sex, tumor size, tumor multiplicity, and tumor grade ($P > 0.05$; Table 1).

Univariate Kaplan–Meier survival analysis demonstrated that clinical outcomes in our patient cohort are representative of those generally observed in BUC, as in our cohort several well-established prognostic parameters had significant impact on patient overall survival (OS) and cancer-specific survival (CSS), including tumor grade (OS: $P = 0.032$, CSS: $P = 0.040$, respectively; Supplementary Table S1), pT classification (OS: $P = 0.004$, CSS: $P = 0.007$, respectively; Supplementary Table S1) and pN classification (OS: $P < 0.001$, CSS: $P < 0.001$, respectively; Supplementary Table S1). Importantly, Kaplan–Meier survival analysis based on REDD1 expression revealed that high REDD1 expression was correlated with poorer OS and CSS of patients with BUC (OS: $P < 0.001$, CSS: $P = 0.001$, respectively; Supplementary Table S1; Fig. 1D and E).

REDD1 expression and other clinical pathological parameters closely related to poor OS and CSS in univariate analysis (tumor grade, pT classification, pN classification) were further examined in multivariate analysis. High REDD1 expression was found to be an independent prognostic factor for poor OS and CSS [OS: HR, 2.772, 95% confidence interval (CI), 1.398–5.497; $P = 0.004$, CSS: HR, 2.005, 95% CI, 0.952–4.223; $P = 0.011$, respectively; Supplementary Table S2]. pT classification (OS: HR, 1.456, 95% CI, 0.973–2.179; $P = 0.041$, CSS: HR, 1.493, 95% CI, 0.949–2.348; $P = 0.023$, respectively; Supplementary Table S2) and pN classification (OS: HR, 2.173, 95% CI, 1.115–4.236; $P = 0.023$, CSS: HR, 2.778, 95% CI, 1.367–5.644; $P = 0.005$, respectively; Supplementary Table S2) were also confirmed to be independent prognostic factors for survival.

REDD1 regulates cell proliferation, apoptosis, and autophagy in BUC cells

As REDD1 is highly expressed in BUC, and its expression is closely related to the prognosis of patients, we further explored the effect of REDD1 on proliferation and apoptosis of BUC cells. We analyzed REDD1 expression in several BUC cell lines (BIU87, 5637, T24, EJ, and RT4). REDD1 expression was high in T24 and EJ cells, which have invasive phenotypes, and low in RT4, BIU87, and 5637 cells, which are poorly invasive (Fig. 2A). To investigate the impact of perturbing REDD1 expression, we knocked REDD1 down in T24 cells (which have high REDD1 expression) using shRNA (Fig. 2B) and overexpressed REDD1 in RT4 cells (which have low REDD1 expression) using an overexpression plasmid (Fig. 2B). The effects of knockdown or overexpression REDD1 on proliferation and apoptosis of BUC cells were detected using CCK-8 and flow cytometry, respectively. Silencing REDD1 expression in T24 cells decreased cell proliferation (Fig. 2B) and increased apoptosis (Fig. 2D). Overexpression of REDD1 in RT4 cells increased cell proliferation (Fig. 2B) and decreased apoptosis (Fig. 2D). Expression of the apoptosis markers cleaved caspase 3 (c-caspase 3) and cleaved PARP (c-PARP) were upregulated after REDD1 knockdown, and downregulated after REDD1 overexpression (Fig. 2F), indicating an inhibitory effect of REDD1 on apoptosis in BUC cells. Cell cycle analysis found that REDD1 knockdown reduces the PI, whereas overexpression of REDD1 increases the PI (Fig. 2E). Expression of the autophagy marker LC3B was higher in T24 cells than in RT4 cells. Moreover, LC3B expression level was downregulated in T24 cells after REDD1 knockdown and upregulated in RT4 cells after REDD1 overexpression (Fig. 2C), suggesting that REDD1 also regulates autophagy in BUC cells. Western blot analysis indicated that LC3-II expression was decreased after REDD1 knockdown and increased after REDD1 overexpression, further indicating the involvement of REDD1 in autophagy (Fig. 2F). Because REDD1 can induce autophagy by activating EEF2K [20], we analyzed EEF2K expression in T24 and RT4 cells. REDD1 overexpression enhanced EEF2K expression, while REDD1 knockdown repressed EEF2K expression (Fig. 2F), suggesting that a "REDD1-EEF2K-autophagy" axis also exists in BUC cells. The results of silencing REDD1 expression in EJ cells and enhancing REDD1 expression in BIU87 cells also demonstrated that REDD1 participates in the regulation of proliferation, apoptosis, and autophagy (Supplementary Fig. S1A–S1F). To further determine the molecular mechanism involved in REDD1 induced EEF2K/autophagy, we extended our observation of mTOR pathway, EEF2K, and autophagy at different time after altering REDD1 expression. We first detected activity of AKT/mTOR pathway in all five cell lines and found that AKT/mTOR pathway activity is higher in T24 and EJ cells but is lower in BIU87 and RT4 cells (Fig. 2A). Then we found that AKT/mTOR pathway is activated early following knockdown-expression of REDD1 in T24 and EJ cells, but recover to normal level at 24 hours. But for EEF2K and

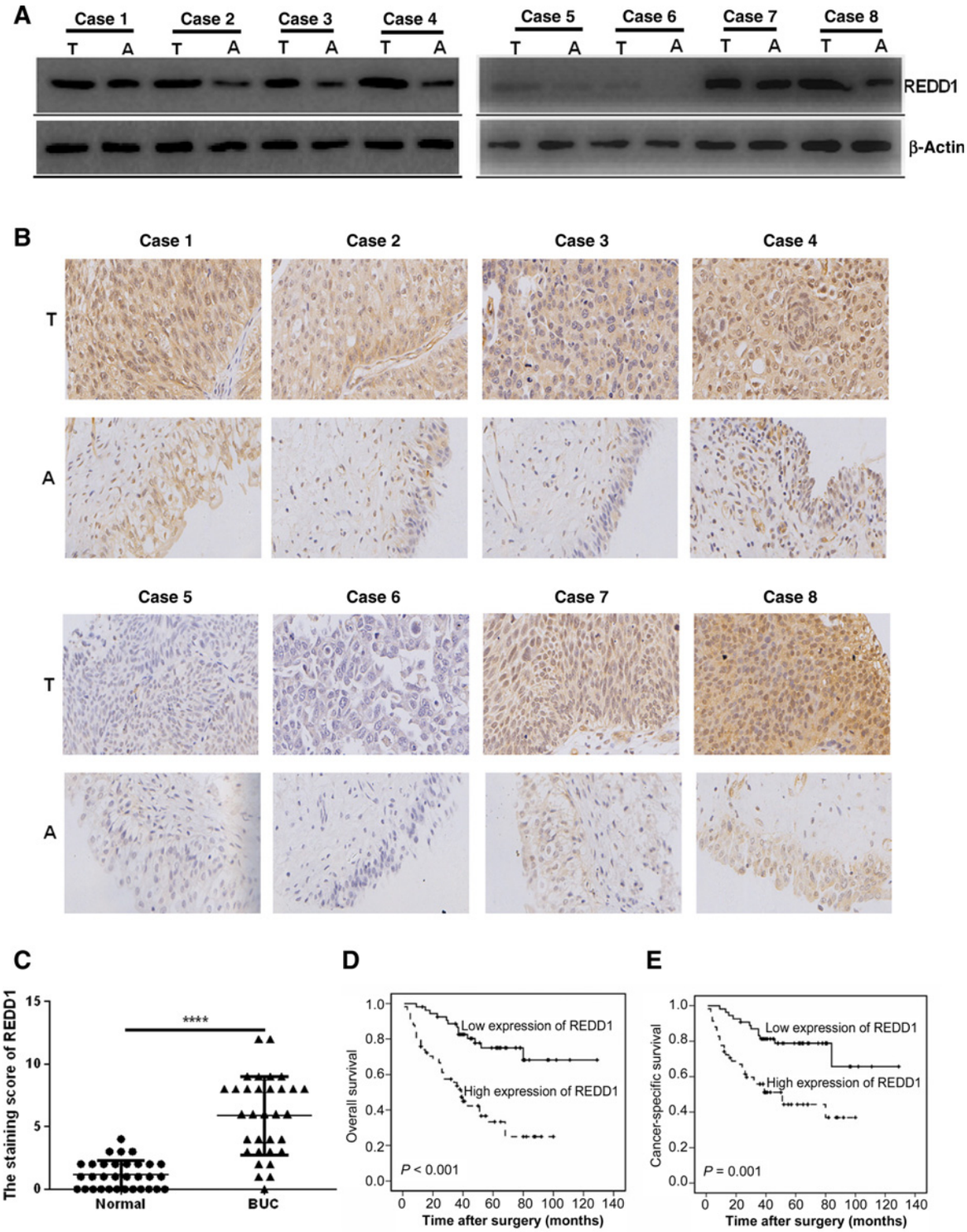

Figure 1.

Increased expression of REDD1 is correlated with poor patient survival. **A,** Western blot analyses of REDD1 protein expression in eight pairs of matched bladder urothelial carcinoma (BUC) tissues; β-actin was used as the loading control. **B,** Representative immunohistochemical analysis of REDD1 expression in parallel on the eight tumor/normal pairs. **C,** Quantification of immunohistochemical analysis of REDD1 expression in 32 primary bladder BUCs and in matched adjacent normal bladder mucosa. **D** and **E,** Kaplan–Meier curves of the OS and CSS of 112 patients with BUC with high or low REDD1 expression. The *P* value was computed by the log-rank test. *T*, tumor tissue; A, adjacent noncancerous bladder urothelial tissue. ****, $P < 0.0001$.

Table 1. Correlation between the clinicopathological features and expression of REDD1 in BUCs

Clinicopathological features	Cases ($n = 112$)	REDD1 protein: Low expression (%) ($n = 54$)	REDD1 protein: High expression (%) ($n = 58$)	*P* value[a]
Age at diagnosis (years)				0.924
≤67[b]	60	32 (53.3)	28 (46.7)	
>67	52	22 (42.4)	20 (47.6)	
Sex				0.444
Male	90	45 (50.0)	45 (50.0)	
Female	22	9 (40.9)	13 (59.1)	
Tumor size (cm)				0.989
≤3.6[c]	58	28 (48.3)	30 (51.7)	
>3.6	54	26 (48.1)	28 (51.9)	
Tumor multiplicity				0.241
Unifocal	35	14 (40.0)	21 (60.0)	
Multifocal	77	40 (51.9)	37 (48.1)	
Tumor grade				0.383
Low	39	21 (53.8)	18 (46.2)	
High	73	33 (45.2)	40 (54.8)	
pT classification				**0.011**
pTa/pT1	31	20 (64.5)	11 (35.5)	
pT2	34	19 (55.9)	15 (44.1)	
pT3/pT4	47	15 (31.9)	32 (68.1)	
pN classification				**<0.001**
pN-	86	51 (59.3)	35 (40.7)	
pN+	26	3 (11.5)	23 (88.5)	

[a]Chi-square test.
[b]Median age.
[c]Median size; BUC, bladder urothelial carcinoma.

autophagy marker, LC3-II, decreased following knockdown-expression of REDD1 in T24 and EJ cells, and reached a lowest level at 24 hours (Fig. 2G; Supplementary Fig. S1G). In contrast, AKT/mTOR pathway are inhibited early following overexpression of REDD1 in BIU87 and RT4 cells, but recover to normal level at 24 hours. Expression of EEF2K and LC3-II increased and reached a highest level at 24 hours following ever-expression of REDD1 in BIU87 and RT4 cells (Fig. 2H and Supplementary Fig. S1H). Those results indicated that REDD1 may activate EEF2K induced autophagy then promote BUC cells survival by inhibiting AKT/mTOR pathway at an early stage. However, the AKT/mTOR pathway recover at later stage through an unclear negative feedback pathway.

Targeted regulation of miR-22 on REDD1 expression

To clarify the mechanisms involved in regulating REDD1 expression in BUC cells, microRNA target prediction databases (microRNA.org and TargetScan) were used to predict miRNAs that could regulate REDD1 expression. Two putative binding sites for miR-22 were identified in the REDD1 3'UTR (Fig. 3A). Expression of miR-22 was assessed in BUC cell lines (BIU87, 5637, T24, EJ, and RT4 cells), and it was found that miR-22 expression was lower in BUC cells with high REDD1 expression (T24 and EJ cells) and was increased in BUC cells with low REDD1 expression (RT4, BIU87, and 5637 cells; Fig. 3B), suggesting an inverse correlation between miR-22 and REDD1 expression. We transfected T24 cells with miR-22 mimics, and silenced miR-22 expression in RT4 cells. Transfection with miR-22 mimic increased miR-22 expression in T24 cells, whereas transfection with anti-miR-22 significantly repressed miR-22 expression in RT4 cells (Fig. 3C). In addition, transfection with miR-22 mimics repressed REDD1 expression in T24 cells, and transfection with anti-miR-22 enhanced REDD1 expression in RT4 cells (Fig. 3D), suggesting that miR-22 can negatively regulate REDD1 expression. We used dual-luciferase experiments to determine if miR-22 can directly regulate REDD1. In HEK293T cells, miR-22 overexpression inhibited the reporter activity of luciferase genes under transcriptional control of wild-type REDD1 3′-UTR (3′-UTR-WT) or of a mutant REDD1 3′-UTR (3′-UTR-MUT2). However, miR-22 did not affect the reporter activity of luciferase with another mutant REDD1 3′-UTR (3′-UTR-MUT1; Fig. 3E), suggesting that the miR-22 binding site is within the region mutated in the 3′-UTR-MUT1 construct. The mutation sites in the REDD1 3'UTR reporter construct are shown in Supplementary Fig. S2A. Moreover, miR-22 levels were inversely correlated with REDD1 expression ($r = -0.5858$, $P = 0.0007$). These data demonstrate that miR-22 directly regulate the expression of REDD1.

miR-22 regulates cell proliferation, apoptosis, and autophagy in BUC cells

Because REDD1 regulates proliferation, apoptosis, and autophagy in BUC cells, and miR-22 directly regulates the expression of REDD1, we determined if miR-22 can also regulate proliferation, apoptosis, and autophagy in BUC cells. Transfection of T24 cells with miR-22 mimics reduced cell proliferation and increased apoptosis, while silencing miR-22 with anti-miR-22 in RT4 cells increased proliferation (Fig. 4A) and reduced apoptosis (Fig. 4B). In addition, perturbing miR-22 expression in T24 or RT4 cells impacted cell-cycle progression (Fig. 4C). The apoptosis markers c-caspase 3 and c-PARP were upregulated after miR-22 overexpression, and downregulated after silencing miR-22 expression (Fig. 4E), suggesting that miR-22 is involved in regulating proliferation and apoptosis in BUC cells. LC3B expression was downregulated after miR-22 overexpression in T24 cells, and upregulated after silencing miR-22 expression in RT4 cells (Fig. 4D); a similar relationship was observed between miR-22 expression and expression of LC3-II (Fig. 4E). The results of enhancing miR-22 expression in EJ cells and silencing miR-22 expression in BIU87 cells also demonstrated that miR-22 participates in the regulation of proliferation, apoptosis, and autophagy in BUC cells (Supplementary Fig. S3–S3E).

Involvement of REDD1 and miR-22 in Taxol chemosensitivity of BUC cells

Both REDD1 and miR-22 have been reported to participate in regulating the chemosensitivity in a variety of cancers (15, 22, 27, 28). However their roles in Taxol-induced cytotoxity in BUC remain unknown. We found that the IC_{25} concentrations of Taxol were 81.46 and 42.87 nmol/L in T24 and RT4 cells, respectively (Supplementary Fig. S2B), indicating that T24 cells with high REDD1 expression are more resistant to Taxol than RT4 cells with low REDD1 expression. To investigate whether REDD1 acts in Taxol-induced cytotoxity of BUC, we transfected T24 or RT4 cells with a REDD1 expression silencing plasmid or a REDD1 overexpression plasmid, respectively, and subsequently treated the cells with their respective IC_{25} concentration of Taxol. Knockdown of REDD1 expression in T24 cells increased Taxol-induced cell cytotoxicity, whereas overexpression of REDD1 reduced Taxol-induced cytotoxicity in RT4 cells (Fig. 5A). We also explored the effect of miR-22 on Taxol-induced cell cytotoxicity in BUC cells. Transfection with

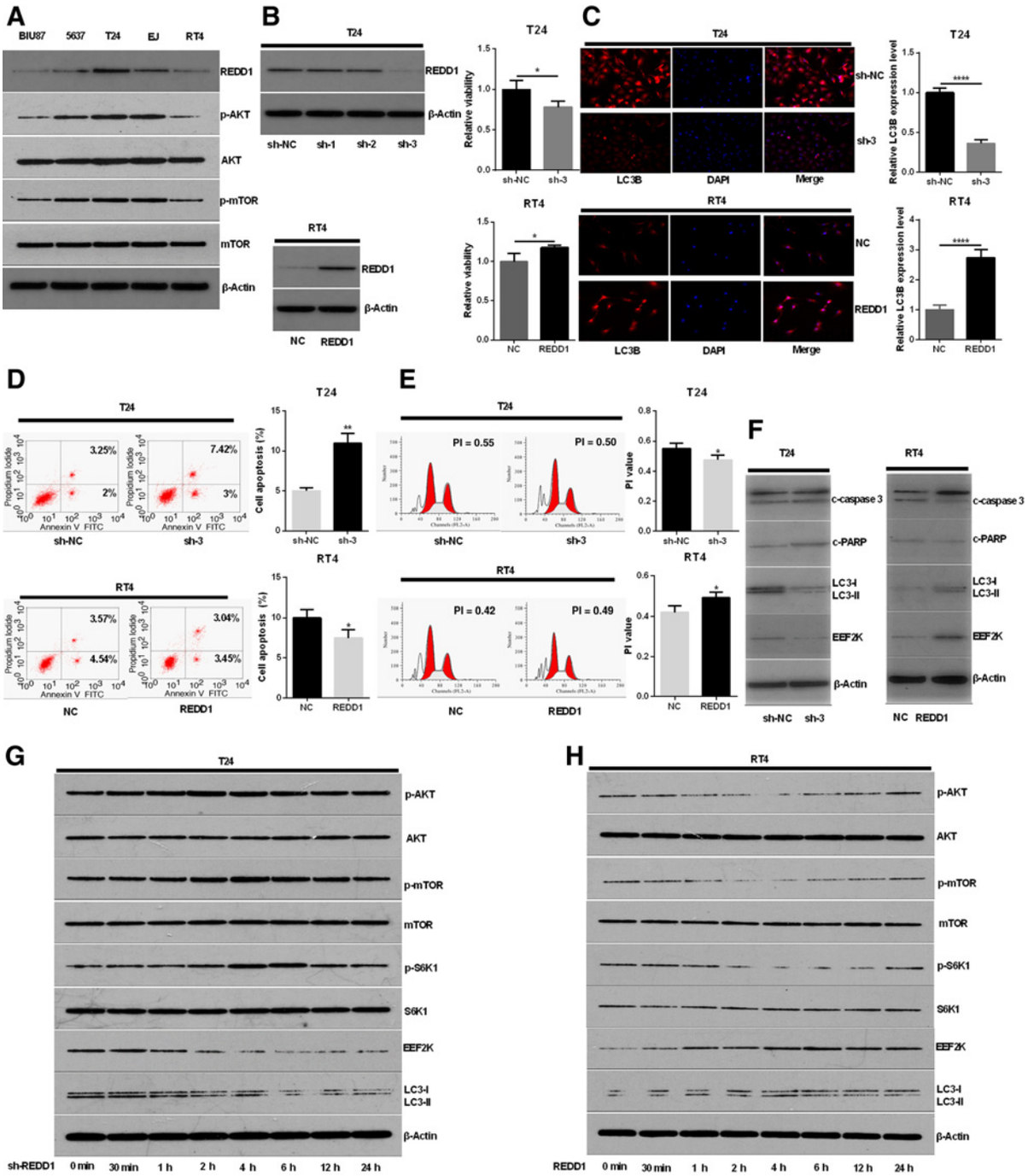

Figure 2.

REDD1 regulates cell proliferation, apoptosis, and autophagy in BUC cells. **A,** Western blot analysis of REDD1 expression and AKT/mTOR signaling in several BUC cell lines (BIU87, 5637, T24, EJ, and RT4). **B,** Western blot analysis of REDD1 in T24 cells transfected with different REDD1-targeting shRNAs (sh-1, sh-2, sh-3), and RT4 cells transfected with REDD1 overexpression plasmid. Cell proliferation was determined in T24 and RT4 cells using the CCK-8 method. **C,** Expression of the autophagy marker LC3B was detected by immunofluorescence, and analyzed with flow cytometry. **D,** Apoptosis of T24 and RT4 cells with modulation of REDD1 expression was detected by flow cytometric analysis of annexin V and propidium iodide staining. **E,** Cell cycle in T24 and RT4 cells was analyzed by flow cytometry analysis. $PI = (S + G_2\text{–}M)/(S + G_2\text{–}M + G_0\text{–}G_1)$. **F,** Protein expression of c-caspase 3, c-PARP, LC3-I/II, and EEF2K after intervention on REDD1 expression was detected by Western blot analysis. **G** and **H**, The levels of p-AKT, AKT, p-mTOR, mTOR, p-S6K1, S6K1, EEF2K, and LC3-I/II were examined by Western blot analysis. The time point of "0 min" was identified beginning at 24 hours after sh-REDD1 or REDD1 plasmid transfecting. ****, $P < 0.0001$; *, $P < 0.05$.

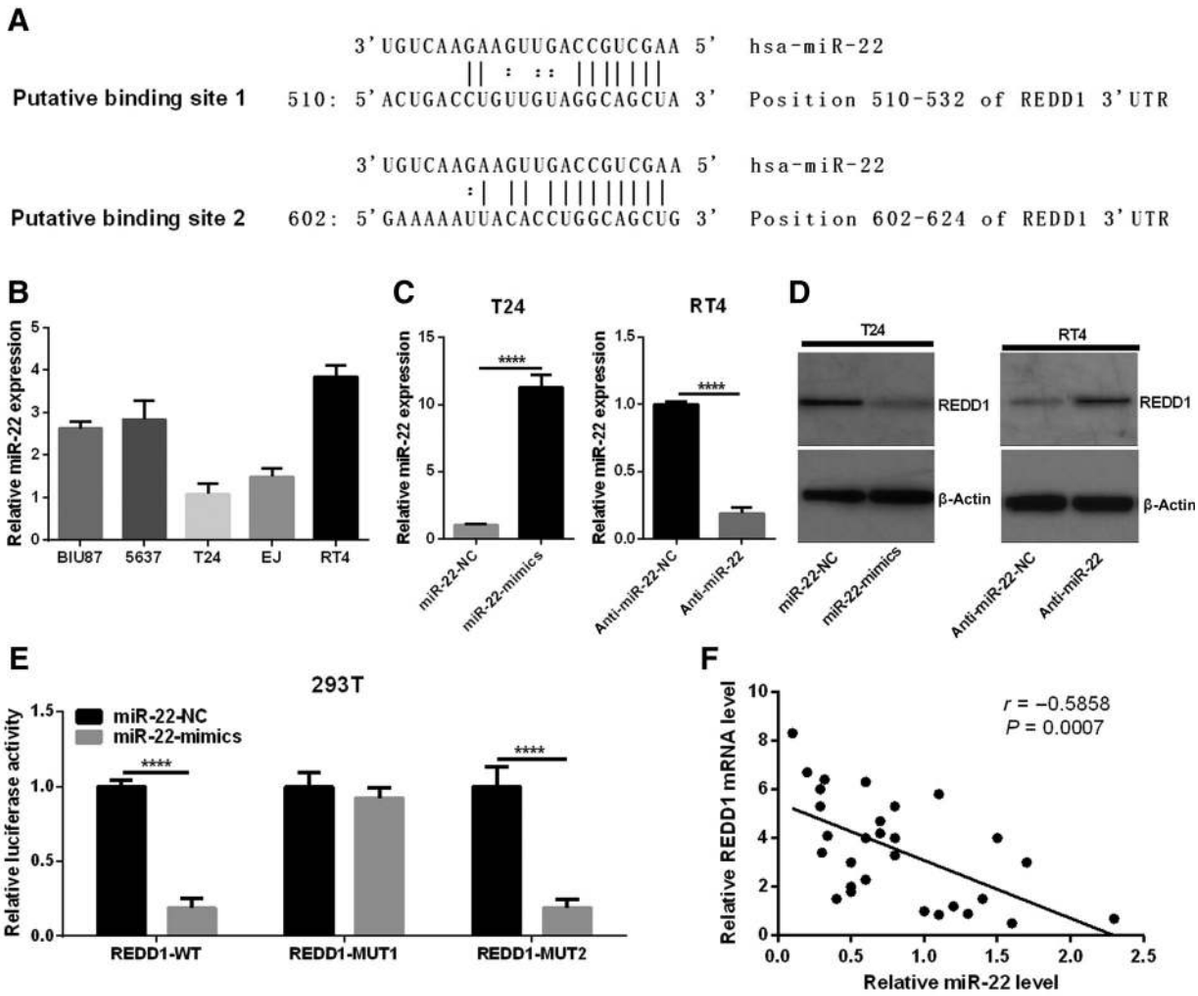

Figure 3.

miR-22 regulates REDD1 expression. **A,** Predicted binding sites for miR-22 within the REDD1 3′UTR (from microRNA.org). **B,** Baseline expression of miR-22 was detected in BIU87, 5637, T24, EJ, and RT4 cells by QRT-PCR. **C,** Expression of miR-22 was detected in T24 or RT4 cells by qRT-PCR after transfection with miR-22 mimics or anti-miR-22, respectively. **D,** REDD1 protein expression was analyzed by Western blot analysis after in T24 or RT4 cells after modulation of miR-22 expression. **E,** Relative luciferase activity from HEK293T cells cotransfected with miR-22 mimics and pMIR-REDD1-3′UTR-WT, pMIR-REDD1-3′UTR-MUT1, or pMIR- REDD1-3′UTR-MUT2. Luciferase activity was detected 48 hours after transfection. **F,** Negative correlation between REDD1 and miR-22 expression in eight pairs of human primary BUC tissues and their corresponding adjacent noncancerous bladder urothelial tissues and additional 14 cases of primary BUC tissues. ****, $P < 0.0001$.

miR-22 mimics increased Taxol-induced cell cytotoxicity in T24 cells, while silencing miR-22 expression suppressed Taxol-induced cytotoxicity in RT4 cells (Fig. 5B). In addition, Taxol-induced apoptosis was increased in T24 cells after knockdown of REDD1 or transfection with miR-22 mimic, as indicated by increases in c-caspase 3 and c-PARP expression (Fig. 5C and D). REDD1 overexpression or silencing of miR-22 in RT4 cells antagonized Taxol-induced c-caspase 3 and c-PARP expression (Fig. 5C and D). These data suggest that REDD1 and miR-22 are involved in Taxol-induced cell apoptosis in BUC cells. Although both REDD1 and miR-22 were shown to regulate autophagy in BUC cells, the single Taxol treatment did not have an obvious impact on autophagy and REDD1 expression (Fig. 5C and D), suggesting that Taxol-induced cytotoxity in BUC is independent of autophagy. However, inhibiting REDD1 or overexpressing miR-22 in BUC cells can repress autophagy, which may synergistically increase Taxol chemosensitivity of BUC cells. Similar involvement of REDD1 and miR-22 in Taxol chemosensitivity upon silencing or enhancing expression of REDD1 and miR-22 were observed in additional EJ and BIU87 cells (Supplementary Fig. S4–SD). Furthermore, to identify the role of autophagy in Taxol chemosensitivity of BUC cells, the autophagy inhibitors 3-MA and CQ were applied to RT4 cells. Both 3-MA and CQ intensified Taxol sensitivity, which was inhibited by REDD1 overexpression plasmid or miR-22 inhibitor (Supplementary Fig. S5A–S5D). These results also indicate that REDD1 regulates proliferation and apoptosis at least partly by autophagy.

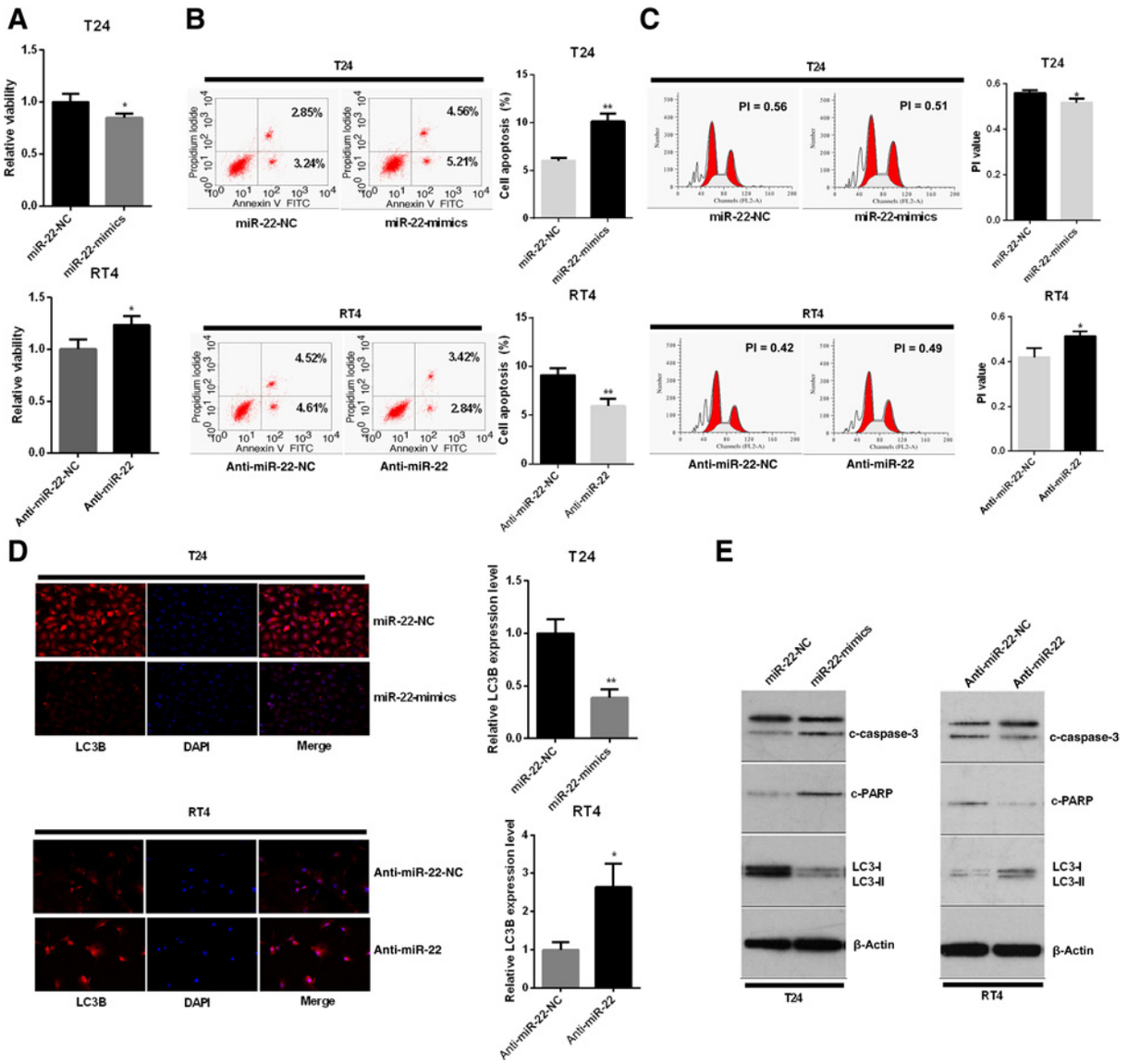

Figure 4.

miR-22 regulates cell proliferation, apoptosis, and autophagy in BUC cells. **A,** T24 cells were transfected with miR-22 mimics, and RT4 cells with miR-22 inhibitors and the CCK-8 method was used to detect cell proliferation. **B,** The effects of miR-22 mimics or inhibitors on apoptosis of T24 or RT4 cells were assessed through annexin V staining and flow cytometry analysis. **C,** Cell cycle was analyzed by flow cytometry. **D,** Immunofluorescence for the autophagy marker LC3B was quantitated with flow cytometry. **E,** Protein expression of c-caspase 3, c-PARP, and LC3-I/II was detected by Western blot after intervention on miR-22 expression. **, $P < 0.01$; *, $P < 0.05$.

Restoration of REDD1 expression counteracts miR-22–mediated Taxol sensitivity

Because both REDD1 and miR-22 modulate Taxol chemosensitivity in BUC cells, and miR-22 directly regulates REDD1 expression, we explored whether the mechanism of miR-22-promoted Taxol chemosensitivity in BUC cells involves repression of REDD1. REDD1 expression was restored in T24 cells transfected with miR-22 mimics by cotransfection with a REDD1 overexpression plasmid. Similarly, REDD1 expression was decreased in RT4 cells transfected with miR-22 inhibitor by cotransfection with a REDD1 silencing plasmid. There was a positive correlation between EEF2K and REDD1 expression changes (Fig. 6A). Compared to transfection with miR-22 mimics, cotransfection with miR-22 mimics and REDD1 overexpression plasmid inhibited Taxol-induced cytotoxicity and Taxol-induced apoptosis in T24 cells (Fig. 6B and C). Compared with the miR-22 inhibitor transfection group, RT4 cells cotransfected with miR-22 inhibitor and REDD1 knockdown vector exhibited increased Taxol-induced cytotoxicity and Taxol-induced apoptosis (Fig. 6B and C). In addition, cotransfection with miR-22 mimics and REDD1 overexpression plasmid restored the decline in autophagy markers caused by miR-22

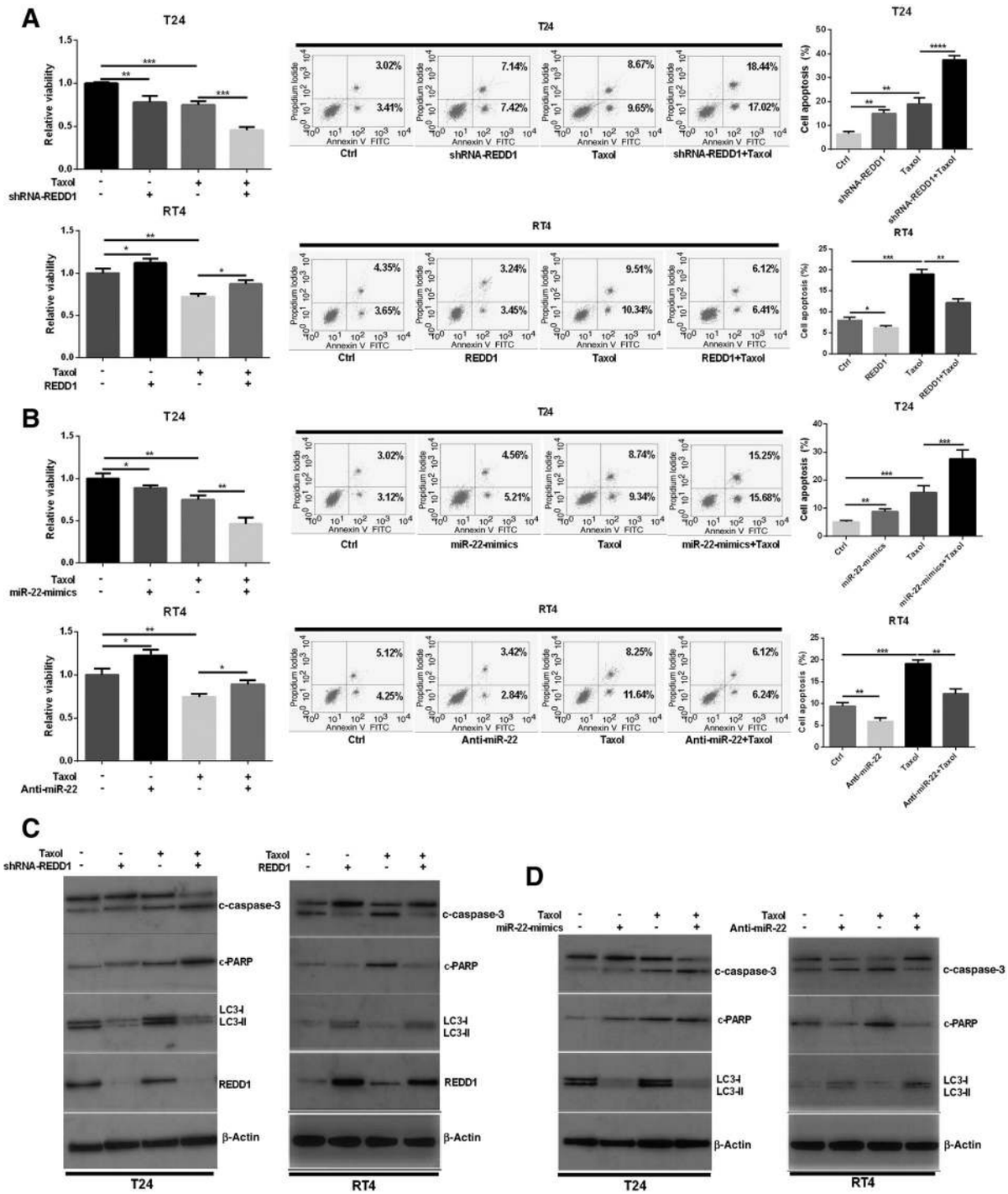

Figure 5.

Involvement of REDD1 and miR-22 in Taxol chemosensitivity in BUC cells. **A** and **B**, The effect of knockdown or overexpression of REDD1 or miR-22 on cell proliferation and apoptosis was examined in T24 and RT4 BUC cells. CCK-8 was used to detect cell proliferation ability, and propidium iodide and annexin V staining were used to detect apoptosis. **C** and **D,** Protein expression of of c-caspase 3, c-PARP, LC3-I/II, and REDD1 were analyzed by Western blot analysis following modulation of REDD1 or miR-22 and/or treatment with Taxol in RT4 and T24 cells.
****, $P < 0.0001$; ***, $P < 0.001$; **, $P < 0.01$; *, $P < 0.05$.

mimics in T24 cells, and cotransfection with miR-22 inhibitor and REDD1 knockdown vector inhibited miR-22 inhibitor-induced autophagy in RT4 cells (Fig. 6A and D). Similar results about restoration of REDD1 expression counteracts miR-22–mediated Taxol sensitivity were observed in EJ and BIU87 cells (Supplementary Fig. S6A–S6D). We found that Taxol significantly inhibited the clone-forming capacity of T24 and RT4 cells (Supplementary Fig. S5E and S5F). Furthermore, transfection of miR-22 mimics in T24 cells increased Taxol-induced inhibition of clone formation, and REDD1 reversed the increase in Taxol-induced inhibition of clone formation due to miR-22 mimics. Transfection of miR-22 inhibitor in RT4 cells inhibited Taxol-induced inhibition of clone formation, and silencing REDD1 reversed the protection of miR-22 inhibitor on RT4 cells (Supplementary Fig. S5E and S5F). These data demonstrate that miR-22 increases Taxol chemosensitivity in BUC cells by directly regulating the expression of REDD1.

Effect of REDD1 on Taxol chemosensitivity in BUC cells *in vivo*

We used a xenograft mouse model to validate the effect of REDD1 on Taxol chemosensitivity of BUC cells *in vivo*. Repression of REDD1 expression with sh-REDD1 plasmid or miR-22 overexpression lentivirus reduced the tumorigenic ability of T24 and EJ cells, and increased Taxol cytotoxicity in the subcutaneous carcinoma model (Fig. 7A and C; Supplementary Fig. S7A and S7C). Upregulation of REDD1 expression with REDD1 overexpression plasmid or anti-miR-22 lentivirus increased the tumorigenic ability of RT4 and BIU87 cells and decreased the cytotoxicity of Taxol in the subcutaneous sarcoma model (Fig. 7B and D; Supplementary Fig. S7B and S7D). In addition, the effect of REDD1 on tumor cells apoptosis was tested by TUNEL assay. Repression of REDD1 expression with sh-REDD1 plasmid or miR-22 overexpression lentivirus markedly increased the apoptosis of T24 and EJ cells, and increased Taxol-induced apoptosis in the subcutaneous carcinoma (Fig. 7E; Supplementary Fig. S7E). Upregulation of REDD1 expression with REDD1 overexpression plasmid or anti-miR-22 lentivirus reduced the apoptosis of RT4 and BIU87 cells and reduced Taxol-induced apoptosis in the subcutaneous carcinoma (Fig. 7F; Supplementary Fig. S7F).

Discussion

Here we report for the first time that REDD1 expression is significantly upregulated in BUC tissue when compared with normal bladder tissue. Moreover, patients with BUC, our clinical analyses revealed the high expression of REDD1 was remarkably correlated to poorer progress in patients with BUC, suggesting that REDD1 may be a potential biomarker to assess prognosis for these individuals.

Recent studies have noted that REDD1 expression is upregulated in several tumor types such as ovarian cancer (18, 19), prostate cancer (20), and colorectal cancer (29). Our results are consistent with those studies. In addition, REDD1 was shown to increase proliferation and decrease apoptosis of BUC cells, suggesting that REDD1 acts as an oncogene in BUC cells.

As a stress-related protein, REDD1 can be stimulated by oxygen deficit, nutrition deficiency, energy stress, and other stress conditions (30). Tumor cells, especially in advanced tumors, are exposed to many kinds of stresses, and REDD1 expression may be a self-protective mechanism of tumor cells to evade apoptosis (20). As an intermediary regulatory link of RAS, HIF-1α, and other oncogenes, REDD1 may inhibit apoptosis and promote tumor progression by activating an anti-apoptotic program (20, 31). Studies found that the survival-promoting mechanisms of REDD1 may involve inhibition of the mTOR signaling pathway (32).

The mTOR signaling pathway regulates the activity of the ULK1 protein activated complex, suppressing autophagy (33). EEF2K is a calcium/calmodulin-dependent enzyme and increases in EEF2K expression can trigger autophagy (13, 34, 35). Studies have found that the mTOR signaling pathway promotes EEF2K degradation through phosphorylating the Ser78/Ser366 site of EEF2K, resulting in decreased autophagy. As an inhibitor of mTOR, REDD1 can stabilize EEF2K expression through the mTOR-EEF2K pathway to promote autophagy (13). Therefore, a REDD1–EEF2K–autophagy regulation axis exists. In this study, both EEF2K expression and autophagy markers were increased after REDD1 overexpression in BUC cells, whereas REDD1 knockout inhibited EEF2K expression and decreased expression of autophagy markers, providing the first evidence for a REDD1–EEF2K–autophagy axis in BUC cells. REDD1-mediated autophagy promotes cell survival (36), and REDD1-promoted autophagy may be one of the mechanisms by which REDD1 acts as an oncogene in BUC.

AKT/mTOR signal pathway has been reported to be activated and to promote BUC cell survival (37). Interestingly, we found higher AKT/mTOR pathway activity in BUC cell lines that express higher REDD1 levels, which seems to be in contrast with the mTOR inhibition role of REDD1. We further found that AKT/mTOR pathway is affected early after REDD1 expression was interrupted but then recover to normal level rapidly, whereas EEF2K induced autophagy was affected at a later stage and sustained for a long time. Of note, REDD1 may activate EEF2K induced autophagy then promote BUC cells survival by inhibiting AKT/mTOR pathway at early stage. However, the AKT/mTOR pathway recovers at later stage through unclear negative feedback pathways. Our finding is in line with the data from Dennis and colleagues, who demonstrated that AKT/mTOR signaling recovered at later stage through a negative feedback loop after REDD1 expression was interrupted in Rat2 fibroblasts (32).

Nucleo-cytoplasmic expression of REDD1 was reported in human neuroblastoma cells and REDD1 protein could be accumulated in the nucleus by treated with Aβ42 (38). Our study also showed that REDD1 is both located in cytoplasm and nucleus in BUC cells. Furthermore, REDD1 tend to be higher concentrated in the cytoplasm in the well differentiated BUC samples and be higher concentrated in the nucleus in the poor differentiated BUC samples (the data was not showed). This phenomenon serves as a reminder that nuclear translocation of REDD1 may contribute to the differentiation of BUC cells. However, further studies are needed to confirm the hypothesis.

Cells can adapt to stress by appropriate activation of autophagy, leading to cell survival. Increased autophagy in tumor cells is a mechanism of tolerance or insensitivity to chemotherapy, and inhibiting the key regulatory molecules of autophagy can effectively enhance chemosensitivity (10, 39). We found that Taxol chemosensitivity was increased after repression of autophagy through silencing REDD1 in T24 cells. In addition, we determined that Taxol chemosensitivity was decreased after upregulating REDD1 in RT4 cells to activate autophagy. Previous studies also reported that inhibiting REDD1–autophagy axis can promote

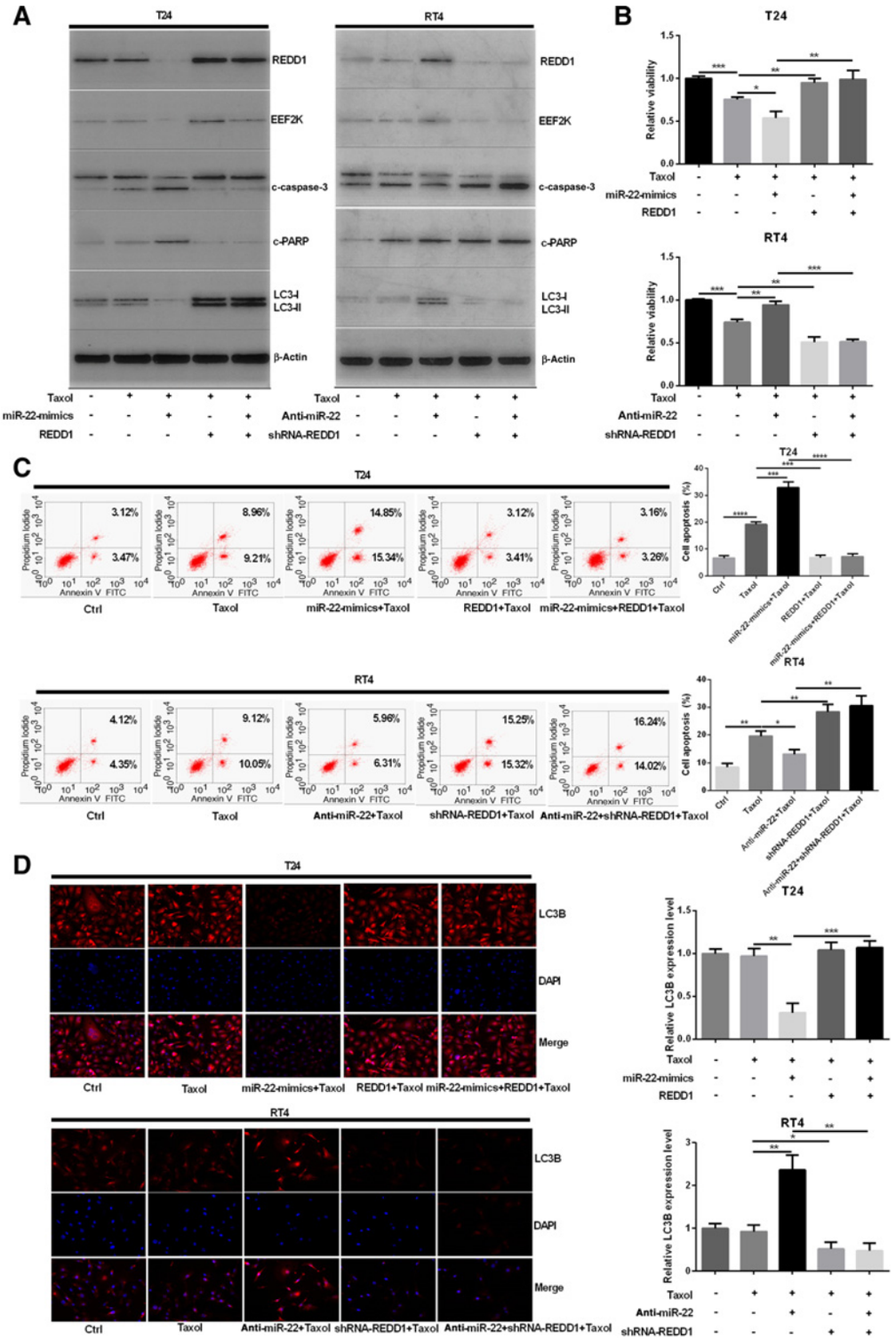

Figure 6.

Restoration of REDD1 expression counteracts miR-22–mediated Taxol sensitivity. T24 and RT4 cells were treated with Taxol and combinations of miR-22 mimics, miR-22 antagonist, shRNA-REDD1, and REDD1 overexpression vector. **A,** Protein expression of c-caspase 3, c-PARP, LC3-I/II, REDD1, and EEF2K was determined by Western blot analysis. **B,** CCK-8 was used to determine treatment effect on cell proliferation. **C,** Flow cytometry was used to detect cell apoptosis. **D,** Autophagy was assessed by immunofluorescence of LCB3 and quantification by flow cytometry. ****, $P < 0.0001$; ***, $P < 0.001$; **, $P < 0.01$; *, $P < 0.05$.

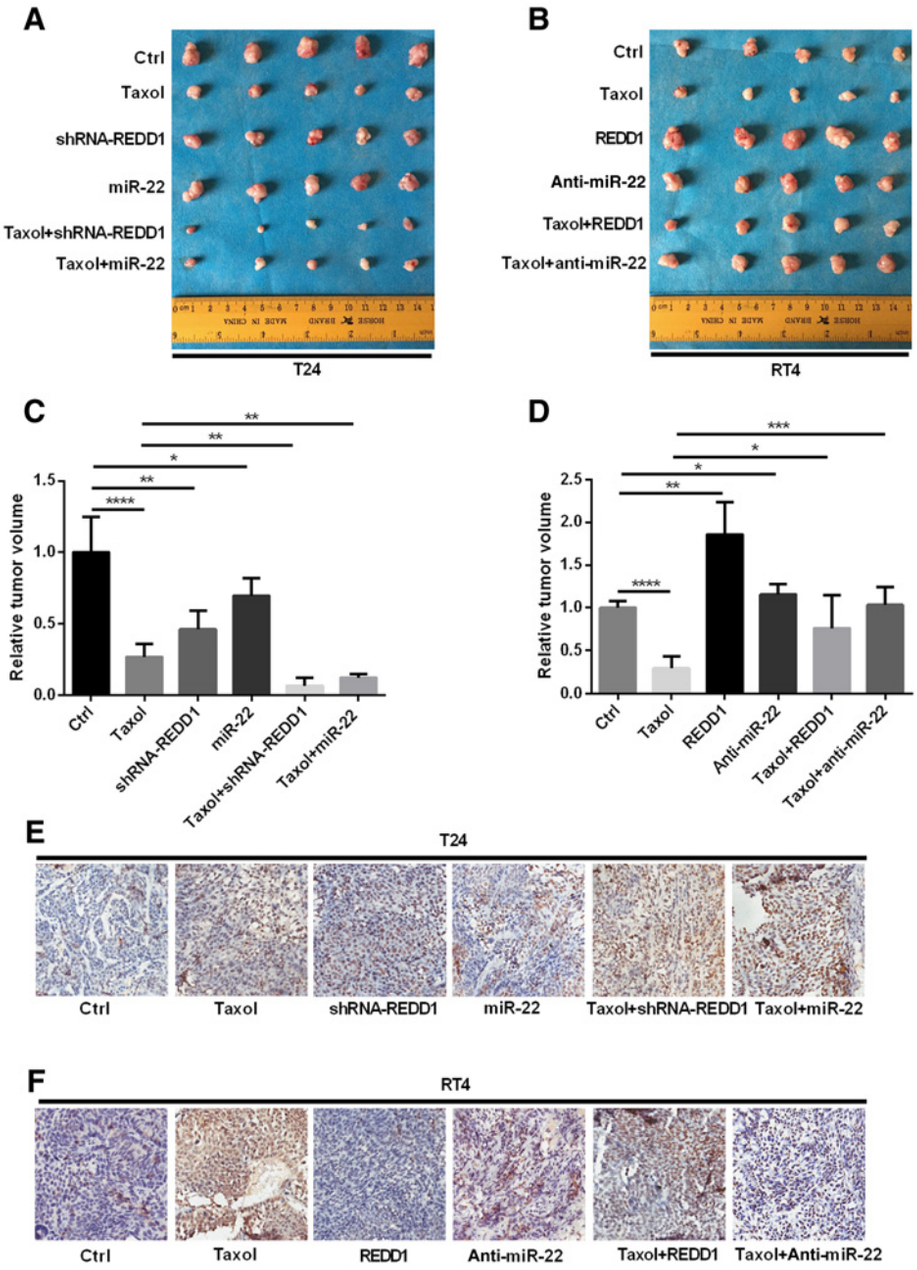

Figure 7.
Effects of REDD1 and miR-22 on Taxol chemosensitivity in T24 and RT4 cells in nude mice. **A** and **B,** Tumor tissues isolated from indicated mice at day 35 posttransplant. **C** and **D,** The tumor volumes were calculated at day 35 posttransplant. **E** and **F,** Tumor cells apoptosis was tested by TUNEL assay. ****, $P < 0.0001$; ***, $P < 0.001$; **, $P < 0.01$; *, $P < 0.05$.

chemosensitivity in myeloma cells (14) and prostate cancer cells (15). In this experiment, Taxol doses at IC_{25} concentrations had no obvious effect on autophagy or REDD1 expression in T24 and RT4 cells (data not presented). Furthermore, it has been reported that Taxol promotes autophagy in ovarian cancer (10) and lung cancer cells (40), but inhibits autophagy in MCF-7 and SK-BR-3 breast cancer cells (41), suggesting that Taxol has different effects on autophagy in different cancer cells. This may be due to differences in the threshold of Taxol-triggered autophagy in a cell-line–specific context. These results indicate that REDD1-mediated autophagy may be a novel target to sensitize BUC cells to Taxol chemotherapy.

REDD1 expression can be induced by MAPK and PKA signaling pathways (42, 43), and can also be negatively regulated by other factors such as Ezrin, T-cell acute leukemia 1 (TAL1), and IL6 (44–46). Here we make the novel discovery that REDD1 is negatively regulated by miR-22. Elevated expression of miR-22 can inhibit the proliferation of BUC cells, increase cell apoptosis, and reduce autophagy. Functional restoration of REDD1 further confirmed the presence of a "miR-22-REDD1-proliferation/apoptosis/autophagy" axis. miR-22 acts as a tumor suppressor gene in many tumors and can participate in regulating the genesis and development of gastric cancer, renal cell carcinoma, liver cancer and other tumors by targeting MMP14, SIRT1, and Gal-9

genes (47–49). Our experiments also demonstrate that miR-22 acts as an anti-oncogene in BUC cells. Furthermore, it has been reported that miR-22 can regulate chemosensitivity in osteosarcoma and colon cancer (27, 28, 50). We confirmed that miR-22 was able to increase chemosensitivity to paclitaxel in BUC cells by inhibiting the REDD1–autophagy axis. The ability of regulating autophagy of miR-22 in BUC cells is coincident with the conclusion in recent studies, which revealed that miR-22 could regulate autophagy by targeting p38α, HMGB1, and BTG1 (27, 51, 52). Finally, this study demonstrated that inhibiting REDD1 expression by RNAi or miR-22 can increase the chemosensitivity of BUC cells to paclitaxel *in vivo*.

In conclusion, REDD1 is highly expressed in BUC tissues, and high expression of REDD1 is an indicator of poor prognosis for patients with BUC. Stimulating or antagonizing the REDD1–EEF2K–autophagy axis can correspondingly increase or decrease the generative capacity of BUC cells. Inhibiting REDD1 expression by RNAi or miR-22 can increase paclitaxel chemosensitivity in BUC cells. Our results demonstrate that REDD1 may be a prognostic biomarker and an actionable target for chemosensitization of BUC.

Disclosure of Potential Conflicts of Interest

No potential conflicts of interest were disclosed.

Authors' Contributions

Conception and design: Q. Zeng, K. Cao
Development of methodology: Q. Zeng, J. Liu, P. Cao, H. Bo, K. Cao
Acquisition of data (provided animals, acquired and managed patients, provided facilities, etc.): Q. Zeng, J. Liu, L. Liu, W. Xiong, J. Li, H. Bo, Y. Zhu, Y. Zhou, Q. Zou, K. Cao
Analysis and interpretation of data (e.g., statistical analysis, biostatistics, computational analysis): Q. Zeng, J. Liu, J. Li, W. Xiong, F. Yang, M. Zhou, Q. Zou, K. Cao
Writing, review, and/or revision of the manuscript: Q. Zeng, J. Liu, P. Cao, J. Li, X. Liu, Y. Cheng, F. Yang, M. Zhou, K. Cao
Administrative, technical, or material support (i.e., reporting or organizing data, constructing databases): Q. Zeng, X. Liu, X. Fan, J. Li, H. Bo, Y. Zhu, J. Hu, Y. Zhou, Q. Zou, J. Zhou, K. Cao
Study supervision: P. Cao, K. Cao
Other (Specify): J. Hu

Acknowledgments

We thank the authors for their excellent work. This work was supported by National Natural Science Foundation of China (Nos. 81572965, 81572689, 81372140), Natural Science Foundation of Hunan Province (2016JJ6154), the Innovation-Driven Project of Central South University (No. 2017CX012), Huxiang Young Talent Project (2016RSRCHX0076), the New Xiangya Talent Projects of the Third Xiangya Hospital of Central South University (20150201, JY201623, JY201615).

The costs of publication of this article were defrayed in part by the payment of page charges. This article must therefore be hereby marked *advertisement* in accordance with 18 U.S.C. Section 1734 solely to indicate this fact.

Received February 17, 2017; revised June 26, 2017; accepted October 24, 2017; published OnlineFirst October 30, 2017.

References

1. Peng M, Huang Y, Tao T, Peng CY, Su Q, Xu W, et al. Metformin and gefitinib cooperate to inhibit bladder cancer growth via both AMPK and EGFR pathways joining at Akt and Erk. Sci Rep 2016;6:28611.
2. Chandrasekar T, Evans CP. Autophagy and urothelial carcinoma of the bladder: a review. Invest Clin Urol 2016;57:S89–S97.
3. Chen W, Zheng R, Baade PD, Zhang S, Zeng H, Bray F, et al. Cancer statistics in China, 2015. CA Cancer J Clin 2016;66:115–32.
4. Rose TL, Milowsky MI. Improving systemic chemotherapy for bladder cancer. Curr Oncol Rep 2016;18:27.
5. Hussain M, Vaishampayan U, Du W, Redman B, Smith DC. Combination paclitaxel, carboplatin, and gemcitabine is an active treatment for advanced urothelial cancer. J Clin Oncol 2001;19:2527–33.
6. Sideris S, Aoun F, Zanaty M, Martinez NC, Latifyan S, Awada A, et al. Efficacy of weekly paclitaxel treatment as a single agent chemotherapy following first-line cisplatin treatment in urothelial bladder cancer. Mol Clin Oncol 2016;4:1063–7.
7. Bellmunt J, von der Maase H, Mead GM, Skoneczna I, De Santis M, Daugaard G, et al. Randomized phase III study comparing paclitaxel/cisplatin/gemcitabine and gemcitabine/cisplatin in patients with locally advanced or metastatic urothelial cancer without prior systemic therapy: EORTC Intergroup Study 30987. J Clin Oncol 2012;30:1107–13.
8. Karam JA, Huang S, Fan J, Stanfield J, Schultz RA, Pong RC, et al. Upregulation of TRAG3 gene in urothelial carcinoma of the bladder. Int J Cancer 2011;128:2823–32.
9. Wang WJ, Li CF, Chu YY, Wang YH, Hour TC, Yen CJ, et al. Inhibition of EGFR/STAT3/CEBPD axis reverses cisplatin cross-resistance with paclitaxel in urothelial carcinoma of urinary bladder. Clin Cancer Res 2017;23:503–13.
10. Zhang SF, Wang XY, Fu ZQ, Peng QH, Zhang JY, Ye F, et al. TXNDC17 promotes paclitaxel resistance via inducing autophagy in ovarian cancer. Autophagy 2015;11:225–38.
11. Ma XH, Piao S, Wang D, McAfee QW, Nathanson KL, Lum JJ, et al. Measurements of tumor cell autophagy predict invasiveness, resistance to chemotherapy, and survival in melanoma. Clin Cancer Res 2011;17:3478–89.
12. Liu C, Xue R, Wu D, Wu L, Chen C, Tan W, et al. REDD1 attenuates cardiac hypertrophy via enhancing autophagy. Biochem Biophys Res Commun 2014;454:215–20.
13. Cheng Y, Ren X, Zhang Y, Shan Y, Huber-Keener KJ, Zhang L, et al. Integrated regulation of autophagy and apoptosis by EEF2K controls cellular fate and modulates the efficacy of curcumin and velcade against tumor cells. Autophagy 2013;9:208–19.
14. Decaux O, Clement M, Magrangeas F, Gouraud W, Charbonnel C, Campion L, et al. Inhibition of mTORC1 activity by REDD1 induction in myeloma cells resistant to bortezomib cytotoxicity. Cancer Sci 2010;101:889–97.
15. Barakat DJ, Mendonca J, Barberi T, Zhang J, Kachhap SK, Paz-Priel I, et al. C/EBPbeta regulates sensitivity to bortezomib in prostate cancer cells by inducing REDD1 and autophagosome-lysosome fusion. Cancer Lett 2016;375:152–61.
16. Kolesnichenko M, Vogt PK. Understanding PLZF: two transcriptional targets, REDD1 and smooth muscle alpha-actin, define new questions in growth control, senescence, self-renewal and tumor suppression. Cell cycle (Georgetown, Tex) 2011;10:771–5.
17. Li XH, Ha CT, Fu D, Xiao M. REDD1 protects osteoblast cells from gamma radiation-induced premature senescence. PloS One 2012;7:e36604.
18. Smith ER, Xu XX. REDD1, a new Ras oncogenic effector. Cell Cycle (Georgetown, Tex) 2009;8:675–6.
19. Jia W, Chang B, Sun L, Zhu H, Pang L, Tao L, et al. REDD1 and p-AKT overexpression may predict poor prognosis in ovarian cancer. Int J Clin Exp Pathol 2014;7:5940–9.
20. Schwarzer R, Tondera D, Arnold W, Giese K, Klippel A, Kaufmann J. REDD1 integrates hypoxia-mediated survival signaling downstream of phosphatidylinositol 3-kinase. Oncogene 2005;24:1138–49.
21. Jin HO, Seo SK, Woo SH, Kim YS, Hong SE, Yi JY, et al. Redd1 inhibits the invasiveness of non-small cell lung cancer cells. Biochem Biophys Res Commun 2011;407:507–11.
22. Yun SM, Woo SH, Oh ST, Hong SE, Choe TB, Ye SK, et al. Melatonin enhances arsenic trioxide-induced cell death via sustained

upregulation of Redd1 expression in breast cancer cells. Mol Cell Endocrinol 2016;422:64–73.
23. Xie B, Cao K, Li J, Chen J, Tang J, Chen X, et al. Hmgb1 inhibits Klotho expression and malignant phenotype in melanoma cells by activating NF-kappaB. Oncotarget 2016;7:80765–82.
24. Zeng Q, Cao K, Liu R, Huang J, Xia K, Tang J, et al. Identification of TDP-43 as an oncogene in melanoma and its function during melanoma pathogenesis. Cancer Biol Ther 2017;18:8–15.
25. Zeng Q, Wang Q, Chen X, Xia K, Tang J, Zhou X, et al. Analysis of lncRNAs expression in UVB-induced stress responses of melanocytes. J Dermatol Sci 2016;81:53–60.
26. Suzuki M, Cao K, Kato S, Komizu Y, Mizutani N, Tanaka K, et al. Targeting ceramide synthase 6-dependent metastasis-prone phenotype in lung cancer cells. J Clin Invest 2016;126:254–65.
27. Zhang H, Tang J, Li C, Kong J, Wang J, Wu Y, et al. MiR-22 regulates 5-FU sensitivity by inhibiting autophagy and promoting apoptosis in colorectal cancer cells. Cancer Lett 2015;356:781–90.
28. Li X, Wang S, Chen Y, Liu G, Yang X. miR-22 targets the 3' UTR of HMGB1 and inhibits the HMGB1-associated autophagy in osteosarcoma cells during chemotherapy. Tumour Biol 2014;35:6021–8.
29. Di Conza G, Trusso Cafarello S, Loroch S, Mennerich D, Deschoemaeker S, Di Matteo M, et al. The mTOR and PP2A pathways regulate PHD2 phosphorylation to fine-tune HIF1α levels and colorectal cancer cell survival under hypoxia. Cell Rep 2017;18:1699–712.
30. Sinha I, Allen JE, Pinto JT, Sinha R. Methylseleninic acid elevates REDD1 and inhibits prostate cancer cell growth despite AKT activation and mTOR dysregulation in hypoxia. Cancer Med 2014;3:252–64.
31. Chang B, Liu G, Yang G, Mercado-Uribe I, Huang M, Liu J. REDD1 is required for RAS-mediated transformation of human ovarian epithelial cells. Cell Cycle (Georgetown, Tex) 2009;8:780–6.
32. Dennis MD, McGhee NK, Jefferson LS, Kimball SR. Regulated in DNA damage and development 1 (REDD1) promotes cell survival during serum deprivation by sustaining repression of signaling through the mechanistic target of rapamycin in complex 1 (mTORC1). Cell Signal 2013;25:2709–16.
33. Alers S, Loffler AS, Wesselborg S, Stork B. Role of AMPK-mTOR-Ulk1/2 in the regulation of autophagy: cross talk, shortcuts, and feedbacks. Mol Cell Biol 2012;32:2–11.
34. Hait WN, Wu H, Jin S, Yang JM. Elongation factor-2 kinase: its role in protein synthesis and autophagy. Autophagy 2006;2:294–6.
35. Cheng Y, Ren X, Zhang Y, Patel R, Sharma A, Wu H, et al. eEF-2 kinase dictates cross-talk between autophagy and apoptosis induced by Akt Inhibition, thereby modulating cytotoxicity of novel Akt inhibitor MK-2206. Cancer Res 2011;71:2654–63.
36. Molitoris JK, McColl KS, Swerdlow S, Matsuyama M, Lam M, Finkel TH, et al. Glucocorticoid elevation of dexamethasone-induced gene 2 (Dig2/RTP801/REDD1) protein mediates autophagy in lymphocytes. J Biol Chem 2011;286:30181–9.
37. Yuge K, Kikuchi E, Hagiwara M, Yasumizu Y, Tanaka N, Kosaka T, et al. Nicotine induces tumor growth and chemoresistance through activation of the PI3K/Akt/mTOR pathway in bladder cancer. Mol Cancer Thera 2015;14:2112–20.
38. Morel M, Couturier J, Pontcharraud R, Gil R, Fauconneau B, Paccalin M, et al. Evidence of molecular links between PKR and mTOR signalling pathways in Abeta neurotoxicity: role of p53, Redd1, and TSC2. Neurobiol Dis 2009;36:151–61.
39. O'Donovan TR, O'Sullivan GC, McKenna SL. Induction of autophagy by drug-resistant esophageal cancer cells promotes their survival and recovery following treatment with chemotherapeutics. Autophagy 2011;7:509–24.
40. Liu F, Liu D, Yang Y, Zhao S. Effect of autophagy inhibition on chemotherapy-induced apoptosis in A549 lung cancer cells. Oncol Lett 2013;5:1261–5.
41. Veldhoen RA, Banman SL, Hemmerling DR, Odsen R, Simmen T, Simmonds AJ, et al. The chemotherapeutic agent paclitaxel inhibits autophagy through two distinct mechanisms that regulate apoptosis. Oncogene 2013;32:736–46.
42. Reuschel EL, Wang J, Shivers DK, Muthumani K, Weiner DB, Ma Z, et al. REDD1 is essential for optimal T cell proliferation and survival. PloS One 2015;10:e0136323.
43. Lee DK, Kim JH, Kim WS, Jeoung D, Lee H, Ha KS, et al. Lipopolysaccharide induction of REDD1 is mediated by two distinct CREB-dependent mechanisms in macrophages. FEBS Lett 2015;589:2859–65.
44. Celik H, Bulut G, Han J, Graham GT, Minas TZ, Conn EJ, et al. Ezrin inhibition upregulates stress response gene expression. J Biol Chem 2016;291:13257–70.
45. Benyoucef A, Calvo J, Renou L, Arcangeli ML, van den Heuvel A, Amsellem S, et al. The SCL/TAL1 transcription factor represses the stress protein DDiT4/REDD1 in human hematopoietic stem/progenitor cells. Stem cells (Dayton, Ohio) 2015;33:2268–79.
46. Pinno J, Bongartz H, Klepsch O, Wundrack N, Poli V, Schaper F, et al. Interleukin-6 influences stress-signalling by reducing the expression of the mTOR-inhibitor REDD1 in a STAT3-dependent manner. Cell Signall 2016;28:907–16.
47. Zuo QF, Cao LY, Yu T, Gong L, Wang LN, Zhao YL, et al. MicroRNA-22 inhibits tumor growth and metastasis in gastric cancer by directly targeting MMP14 and Snail. Cell Death Dis 2015;6:e2000.
48. Zhang S, Zhang D, Yi C, Wang Y, Wang H, Wang J. MicroRNA-22 functions as a tumor suppressor by targeting SIRT1 in renal cell carcinoma. Oncol Rep 2016;35:559–67.
49. Yang Q, Jiang W, Zhuang C, Geng Z, Hou C, Huang D, et al. microRNA-22 downregulation of galectin-9 influences lymphocyte apoptosis and tumor cell proliferation in liver cancer. Oncol Rep 2015;34:1771–8.
50. Li J, Zhang Y, Zhao J, Kong F, Chen Y. Overexpression of miR-22 reverses paclitaxel-induced chemoresistance through activation of PTEN signaling in p53-mutated colon cancer cells. Mol Cell Biochem 2011;357:31–8.
51. Guo S, Bai R, Liu W, Zhao A, Zhao Z, Wang Y, et al. miR-22 inhibits osteosarcoma cell proliferation and migration by targeting HMGB1 and inhibiting HMGB1-mediated autophagy. Tumour Biol 2014;35:7025–34.
52. Li G, Wang G, Ma L, Guo J, Song J, Ma L, et al. miR-22 regulates starvation-induced autophagy and apoptosis in cardiomyocytes by targeting p38alpha. Biochem Biophys Res Commun 2016;478:1165–72.